Available at www.sciencedirect.com

ScienceDirect

journal homepage: www.elsevier.com/locate/issn/15375110

Research paper: PA—Precision Agriculture

Sensor fusion for improving the estimation of roll and pitch for an agricultural sprayer

L.R. Khot[a], L. Tang[a,*], B.L. Steward[a], S. Han[b]

[a]Agricultural and Biosystems Engineering, 100 Davidson Hall, Iowa State University, Ames, IA 50011, USA
[b]John Deere Ag Management Solutions, 4140 114th Street, Urbandale, IA 50322, USA

ARTICLE INFO

Article history:
Received 12 June 2007
Received in revised form
19 May 2008
Accepted 23 May 2008
Available online 30 July 2008

Sensor fusion using a Discrete Kalman Filter (DKF) was applied to integrate the attitude angle estimates obtained from a Digital Elevation Model (DEM) and a Terrain Compensation Module (TCM) sensor to improve the roll and pitch angle estimates of a self-propelled sprayer. Vehicle attitude and field elevation were measured at two speeds (5.6 and 9.6 km h^{-1}), using a self-propelled agricultural sprayer equipped with Real-Time Kinematic-Differential Global Positioning System (RTK-DGPS) receiver, a TCM sensor and an Inertial Measurement Unit (IMU). The DKF-, DEM-based roll and pitch estimates, the TCM sensor roll and the GPS-based pitch estimates were compared with the reference IMU measurements to validate the performance of the fusion algorithm. A second order autoregressive (AR) model was developed to model the irregular spiked noise in TCM roll and high-frequency noise in GPS-based pitch angle estimates.

The AR modelled error states were incorporated into the DKF algorithm and the measurement noise covariance was estimated from the AR model, which limited the fine tuning of noise covariance to the process noise covariance only. The DKF was able to overcome the out-of-bound situation (data outage) in DEM while it estimated the attitude of the self-propelled sprayer. Additionally, the fusion algorithm was proven to be effective in improving attitude estimate of the self-propelled agricultural sprayer, which can be extended to facilitate the automatic control of the implements that interact with the soil surface on an undulating topographic surface.

Published by Elsevier Ltd on behalf of IAgrE.

1. Introduction

Agricultural vehicle navigation sensors that are available in the market can provide the position and heading of an automated vehicle. This is useful for localisation as well as for steering control of the vehicle. Under rough terrain conditions, knowing the precise attitude of the vehicle together with vehicle speed and soil conditions can provide greater control of autonomous agricultural vehicles steerability (Reid *et al.*, 2000), and also help to prevent rollover of the vehicles operating in uphill/downhill conditions (Kise and Zhang, 2006). Similarly, knowledge of vehicle attitude could also greatly facilitate automatic operational control of the equipments during precision farming.

Digital Elevation Models (DEMs) are often used to model terrain surfaces to procure important physical information

* *Corresponding author.*
E-mail addresses: lietang@iastate.edu (L. Tang), hanshufeng@johndeere.com (S. Han).
1537-5110/$ – see front matter Published by Elsevier Ltd on behalf of IAgrE.
doi:10.1016/j.biosystemseng.2008.05.015

about the field terrain conditions. DEMs are used to determine terrain attributes such as slope and aspect, drainage basins, watershed features, peaks, pits and other landforms for hydrological modelling. Global Positioning System (GPS) technology is one of the several technologies which are employed to collect topographic data and construct DEMs and topographic maps (Colvocoresses, 1993; Yao and Clark, 2000). Clark and Lee (1998) compared the stop-and-go GPS data collection (collecting data from point to point) with kinematic GPS data collection (collecting data continuously with a fixed time step), and found that the kinematic data collection is a more viable method for rapidly developing topographic maps with high elevation accuracy. The single frequency GPS receiver provides reasonably accurate DEMs with elevation error of 100–120 mm for 10 or more passes of the data (Yao and Clark, 2000). Westphalen *et al.* (2004) evaluated DEMs developed by two different methods: (1) considering the elevation measurements only, and (2) combining the elevation and vehicle attitude measurements. In their research, the elevation and vehicle attitude measurements of a self-propelled agricultural sprayer were obtained from four Real-Time Kinematic-Differential Global Positioning System (RTK-DGPS) receivers and an Inertial Measurement Unit (IMU). The DEM developed by combining the elevation with the vehicle attitude measurements had a Root Mean Square Error (RMSE) of 100–110 mm compared to an RMSE of 150 mm for the DEM developed using the elevation measurements alone. Thus, DEMs developed using both elevation measurements and attitude measurements of the vehicle can be useful in improving the attitude estimates of the vehicle travelling in the same terrain field. In particular, vehicle attitude, roll and pitch angle estimates, could be improved using DEMs. Improved attitude estimates for vehicles equipped with steering controllers could allow for better in-field steering and improved control of equipment.

The Discrete Kalman Filter (DKF) is an effective algorithm capable of combining measurements from complimentary sensors for linear system states estimation. Guo *et al.* (2003) developed a Position–Velocity–Attitude (PVA) model-based Kalman filter to estimate an accurate and robust vehicle positioning for precision farming applications. Barut *et al.* (2007) used an Extended Kalman Filter (EKF) to minimize the transient and steady state estimate errors within different velocity ranges. Kallapur and Anavatti (2006) found EKF applicable in estimating the state and parameters of an unmanned aerial vehicle with three dynamic models. Hong *et al.* (1998) implemented EKF algorithm to reduce attitude errors, in order to use a strap-down Attitude Reference System (ARS) in preference to high-cost Inertial Navigational System (INS) for underwater vehicle navigation. Rehbinder and Hu (2000) compared a high gain observer algorithm and EKF algorithm for their accuracy in estimating pitch and roll for walking robot. The data was collected from rate gyroscopes and inclinometers. It was concluded that the high gain observer performed slightly better than EKF. However, it was also suggested that the possible reason for lower performance of EKF could be the complications involved in fine tuning of the EKF. For these reasons the EKF was not implemented in this study.

In the present study, a new approach using DEM for estimating the roll and pitch angles of an agricultural sprayer vehicle has been employed. DEM-based attitude of the vehicle was used to complement the attitude estimates obtained from sensors such as Terrain Compensation Module (TCM) and RTK-GPS. Vehicle attitude estimates obtained from DEM, roll measurements received from the TCM sensor and pitch estimates derived from RTK-GPS signal of a self-propelled sprayer were integrated using DKF to improve roll and pitch angle estimates. In vehicle localisation and navigation, angular rate gyroscopes, magnetometers, digital compass and accelerometers are commonly used to determine the attitude of a vehicle (Wang and Gao, 2005; Xiang and Ozguner, 2005; Khot *et al.*, 2006). The TCM sensor (Deere & Co., Moline, IL, USA) used in present study corrects the vehicle position under the side slope conditions, based on the measured roll angles of the vehicle. However, TCM sensor measurements have high-frequency noise associated with roll measurements. The pitch angle of the vehicle estimated from single RTK-GPS receiver also has noise associated with it, due to the propagation of errors in the GPS measurements. The sensor fusion algorithm implemented in the present study was expected to enhance the vehicle attitude estimates by reducing the high frequency noise associated with TCM sensor as well as the roll and pitch estimation errors in the DEM. The DEM estimated attitude of a sprayer sometimes suffers from out-of-bound situation, where no attitude estimates are available. In such situations, DKF was also expected to provide the attitude estimates using complimentary sensors in the fusion process. Therefore, the major objectives of this research were (1) to develop and implement a DKF sensor fusion algorithm that combines attitude estimates from DEM, TCM and GPS to improve the roll and pitch estimates of a self-propelled sprayer; and (2) to have accurate attitude estimates of a vehicle even when the out-of-bound situation prevails in the vehicle path that restricts access to DEM-based estimates.

2. Methodology

Data was collected from a small field located west of Ames, Iowa, USA, using a John Deere self-propelled sprayer (Model 4710, Deere & Co., Moline, IL, USA). The field had a total area of 0.22 ha (36.58 m wide and 60.96 m long). The sprayer was equipped with an IMU (model VG600AA-201, Crossbow Technology Inc., San Jose, CA, USA), an RTK-GPS receiver (StarFire RTK, Deere & Co., Moline, IL, USA) and a TCM sensor. The TCM sensor along with the GPS receiver was mounted on the top front of the vehicle cab at a distance of 1.93 m from the centre of the cabin. The RTK-GPS receiver was mounted on the left side of the cabin, 1.63 m from front end and 1.53 m from the centre. The sprayer was operated at two speeds: 5.6 km h^{-1} (low speed) and 9.6 km h^{-1} (medium speed); and the datasets were collected at a sampling frequency of 5 Hz. In order to avoid data clustering at a few angles, and to obtain well-distributed data across the entire field range, the field area was traversed at various orientations (e.g. along the main slope, perpendicular to the main slope and at 45° to the main slope) so that the vehicle

would experience a range of attitude angles during the data acquisition.

2.1. Sources of sensor errors

The reference IMU used in the present study was a high-end solid state inertial measurement sensor with fibre optics vertical gyros (Crossbow Technology Inc., San Jose, CA, USA). The roll and pitch angle measurements from IMU sensor were used as reference measurements to validate the effectiveness of the developed DKF algorithm. The implication was that IMUs provide angle measurements with lesser variation and drift compared to conventional inertial measurement systems. The errors from DKF and DEM estimated roll and pitch were calculated by subtracting respective roll and pitch angle estimates from the reference IMU measurements. The error modelling was carried out on the error from TCM roll measurements and GPS-based pitch estimates obtained by subtracting the respective angle measurements from IMU measurements.

Several potential sources of errors existed when estimating the roll and pitch angles of the agricultural sprayer vehicle using DEMs. Firstly, it was found that the sprayer occasionally travelled in area of the field for which there was no valid DEM data. Secondly, during experimental runs the sprayer vehicle interacted with small scale variations caused by micro-topography of the field surface which were probably not captured in the DEM. Thirdly, the RTK-GPS had elevation measurement errors which were propagated into the DEMs. In case of TCM sensor, the roll measurements followed the IMU measurements but with sudden abrupt spikes. The errors in TCM data increased in magnitude with increasing travel speed. The pitch angle estimates from single RTK-GPS receiver mounted on the sprayer were noisy as the errors in the RTK-GPS position and elevation measurements propagated into the pitch angle calculations.

In the fusion process, these sensor errors need to be modelled using an appropriate error modelling technique to improve the performance of the DKF, which is based on the assumption that the noise is white and Gaussian. Thus, the measurement error of the roll angle obtained from the TCM sensor and the error of the pitch angle estimated from a single GPS receiver were modelled using an autoregressive (AR) error modelling technique.

2.2. AR error model

AR modelling, which is common for time series analysis, uses a weighted linear combination of past input samples to predict the current input sample (Babu and Wang, 2004). In the present research, AR modelling was used to standardise the sensor measurement noise so that it can be better described as a white Gaussian noise, an intrinsic assumption of the Kalman filter theory. In many studies where Kalman filters were implemented, researchers had to manually fine tune the system (Q) and measurement noise covariance (R) matrices to obtain optimum Kalman state estimates (Bergeijk *et al.*, 1998; Kiriy and Buehler, 2002). Fine tuning of both Q and R is basically a trial-and-error process which is difficult to use practically, especially when multiple sensor measurements and multiple state variables are incorporated into the Kalman filter design. Although it is difficult to compute the system noise covariance, the measurement noise covariance can be computed if the reference measurements for the different onboard sensors of the system are available. Sensor measurements can have errors depending on the sensor characteristics. To account for sensor measurement errors in the fusion process, the AR modelling technique was applied in this research. This conferred a zero mean white Gaussian noise to the DKF implementation, as well as provided inputs to a measurement noise covariance R.

The AR process used to model a time series (y_t) is

$$y_t = A_1 y_{t-1} + \cdots + A_p y_{t-p} + \varepsilon_t \quad (1)$$

where, A_1 to A_p are the coefficients of AR model with order p ($p <$ length of time series under investigation) and ε_t is uncorrelated random noise with zero mean and variance (σ^2). The determination of an appropriate AR model involves a number of interrelated problems such as the selection of a suitable order and estimation of the coefficients of the AR model. Some of the most commonly used criteria for selecting the order and for obtaining the AR model coefficients are the Final Prediction Error (FPE), Akaike Information Criterion (AIC), Bias Corrected AIC or Akaike's Information Corrected Criterion (AICC), Bayesian Information Criterion (BIC), Minimal Descriptive Length (MDL), φ Criterion, Haring (HAR) criterion, and Jenkins and Watts (JEW) criterion (Djuric and Kay, 1993; Babu and Wang, 2004; Broersen and De Waele, 2005). Liew (2004) found that FPE, AIC, Schwarz Information Criterion (SIC) and BIC criteria perform considerably better when estimating the true order of an AR model for small number of samples. For further information on the AR model order selection criteria, readers are referred to Brockwell and Davis (1996). The modelling of the estimates of roll and pitch angle using the above-mentioned criteria suggested second order models for the roll and pitch measurements of the low and medium speed data. However, the JEW criterion suggested a fifth order model on the same data. Second order models were obtained using FPE order selection criterion and this order was used with Burg's method to get the AR model coefficients.

2.3. Kalman filter implementation

The Kalman filter is an extremely effective and versatile procedure for combining noisy sensor outputs to estimate the state of a system with uncertain dynamics (Grewal *et al.*, 2001). A DKF can estimate the linear dynamic system states that can only be observed indirectly or inaccurately by the system itself. The system state is defined as the minimum information about the past and the present, required to determine an optimal estimate of the future response using the future noisy measurements (Padulo and Arbib, 1974; Woods and Radewan, 1977).

Kalman filter estimation of the state improves as the number of processed measurements increases. To get a quality state vector, Wang (1998) used a 2D Kalman filter twice with the same noisy DEM data using different orientations to estimate the terrain variables from the DEM. This filtering approach reduced the standard deviation of the random noise

from the DEMs by 70% for the elevation and 85% for the first partial derivatives of the elevation.

In this research, the DKF algorithm was applied to improve the sprayer attitude angle estimates. In order to improve the quality of the estimation process, a Kalman filter was applied on the same datasets twice; firstly in the forward direction and secondly in the reverse direction (Wang, 1998); and the average of the two estimated states were used as the final estimated states of our interest. The roll and pitch angle estimates of the self-propelled sprayer from DEMs were fused with the roll measurements from the TCM and pitch estimates from the GPS. The system state vector used in this process is defined as

$$x_k = \left[\phi_k, \theta_k, \phi_{err1_k}, \phi_{err2_k}, \theta_{err1_k}, \theta_{err2_k}\right]^T \quad (2)$$

where, ϕ and θ are the roll and pitch angles with ϕ_{err1}, ϕ_{err2} and θ_{err1}, θ_{err2} corresponding to roll and pitch angle error states, respectively. The error states were obtained from the AR error model. Second order AR model based on FPE order selection criterion was found to be optimum for the TCM roll and GPS-based pitch angle errors that were calculated using corresponding IMU measurements as the reference. Therefore, in the formulated state space equations, each order corresponded to an individual error state.

The above states are represented by the following system function, $f(x)$:

$$f(x) = \left[f_\phi, f_\theta, f_{\phi_{err1}}, f_{\phi_{err2}}, f_{\theta_{err1}}, f_{\theta_{err2}}\right]^T \quad (3)$$

Each system function is characterised by the kinematic equations (Eqs. (4) and (5)) for the roll and pitch angle estimates of the sprayer along with the error estimates (Eqs. (6)–(9)) from these angles using a DKF algorithm.

$$f_\phi = \phi_{k+1} = \phi_k + \dot{\phi}_k \Delta T + \varepsilon_\phi \quad (4)$$

$$f_\theta = \theta_{k+1} = \theta_k + \dot{\theta}_k \Delta T + \varepsilon_\theta \quad (5)$$

$$f_{\phi_{err1}} = \phi_{err1,k+1} = A_{\phi 1}\phi_{err,k} \quad (6)$$

$$f_{\phi_{err2}} = \phi_{err2,k+1} = A_{\phi 2}\phi_{err,k-1} \quad (7)$$

$$f_{\theta_{err1}} = \theta_{err1,k+1} = A_{\theta 1}\theta_{err,k} \quad (8)$$

$$f_{\theta_{err2}} = \theta_{err2,k+1} = A_{\theta 2}\theta_{err,k-1} \quad (9)$$

where, $k+1$, k and $k-1$ are future, present and previous time steps, respectively; ΔT is sampling interval (s); $\dot{\phi}$ and $\dot{\theta}$ are the roll and pitch rates from the DEM; $A_{\phi 1}$, $A_{\phi 2}$, $A_{\theta 1}$ and $A_{\theta 2}$ are the AR coefficients for the roll and pitch error estimation, respectively; ε_ϕ and ε_θ are the random white Gaussian noise for roll and pitch. The estimated roll and pitch angle states at $k+1$ time step were subtracted from the corresponding TCM roll and GPS-based pitch estimates to get the initial roll (ϕ_{err}) and pitch (θ_{err}) angle error. The roll and pitch errors obtained at time step k and $k-1$ using the above method were then used to estimate the error states (Eqs. (6)–(9)) along with the AR model coefficients. The estimated error states were added to get the roll and pitch angle error state vector.

The system matrix (A_k) relating the previous state to the present system state x_k (Eq. (2)) is

$$A_k = \begin{pmatrix} 1 & 0 & 0 & 0 & 0 & 0 \\ 0 & 1 & 0 & 0 & 0 & 0 \\ 0 & 0 & A_{\phi 1} & 0 & 0 & 0 \\ 0 & 0 & 0 & A_{\phi 2} & 0 & 0 \\ 0 & 0 & 0 & 0 & A_{\theta 1} & 0 \\ 0 & 0 & 0 & 0 & 0 & A_{\theta 2} \end{pmatrix}_{x_k} \quad (10)$$

The DEM estimated roll, pitch rates used in system kinematic equations (Eqs. (4) and (5)) were taken as the control inputs $u_k = [\dot{\phi}\ \dot{\theta}]^T$. The input matrix ($B_k$) was then derived by taking partial derivatives of system function $f(x)$ (Eq. (3)) with respect to these control inputs.

$$B_k = \begin{pmatrix} \Delta T & 0 \\ 0 & \Delta T \\ 0 & 0 \\ 0 & 0 \\ 0 & 0 \\ 0 & 0 \end{pmatrix}_{x_k} \quad (11)$$

The measurement vector (Eq. (12)) consisted of the roll angle measurements from the TCM and the pitch angles derived from a single RTK-GPS antenna mounted on the front of the self-propelled sprayer. The roll and pitch angle errors from these measurements were modelled using the AR modelling technique as discussed in Section 2.2. Errors as estimated by the DKF error states were then subtracted from the measurement vector (z_k) before using these measurements to calculate the DKF estimates of the roll and pitch angles.

$$z_k = [\phi_{TCM} - \phi_{err1}k - \phi_{err2}k, \theta_{GPS} - \theta_{err1}k - \theta_{err2}k]^T \quad (12)$$

The measurement matrix (H_k) which relates the measurements (Eq. (12)) with the system states of our interest (Eq. (2)) was derived as below

$$H_k = \begin{pmatrix} 1 & 0 & -1 & -1 & 0 & 0 \\ 0 & 1 & 0 & 0 & -1 & -1 \end{pmatrix}_k \quad (13)$$

3. Results and discussion

The Kalman filter was implemented on the roll and pitch datasets collected at two speeds: 5.6 km h^{-1} (low speed) and 9.6 km h^{-1} (medium speed). The latitude and longitude measurements from the RTK-GPS receiver were converted to the Universal Transverse Mercator (UTM) coordinates. These UTM and the heading angle measurements from the GPS were then used to obtain the UTM coordinate positions of each of the four wheels of the self-propelled sprayer. The four wheel positions and elevation of each wheel obtained from the DEM along with static vehicle measurements were used to estimate the roll and pitch angles of the self-propelled sprayer. The second order AR model based on various order selection techniques was used to model the roll measurements from the TCM sensor and also to model the GPS-based pitch estimates. AR model coefficients were obtained for the second order AR model using Burg's method (Table 1). The AR coefficients on the low-speed TCM data for error modelling showed that the model gave a higher weight to the $k-1$ sample compared to $k-2$ sample while predicting the present (k) sample. The same trend was observed for the GPS-based pitch error modelling.

The model coefficients were used to estimate the error from the roll and pitch angle measurements so that the

Table 1 – AR model coefficients for roll and pitch angle using second order AR model; where $A_{\phi 1}$ and $A_{\phi 2}$ are roll error estimates, $A_{\theta 1}$ and $A_{\theta 2}$ are pitch error estimates, and Err_{ϕ} and Err_{θ} are residual errors in roll and pitch

Sprayer path	Coefficients for roll		Coefficients for pitch		Residual error (°)	
	$A_{\phi 1}$	$A_{\phi 2}$	$A_{\theta 1}$	$A_{\theta 2}$	Roll (Err_{ϕ})	Pitch (Err_{θ})
Low speed	0.591	0.345	0.991	0.090	1.120e−4	1.231e−4
Medium speed	0.754	0.122	0.857	0.006	3.801e−4	3.037e−4

Gaussian residue of the noise could be separated from the other sources of errors in the angle measurements. The Kurtosis analysis before and after AR modelling was performed on the roll and pitch error and its residuals. The original roll and pitch error distributions had Kurtosis values greater than three meaning that the error distribution always reached a peak. The residual error following AR modelling of roll and pitch error showed Kurtosis statistics close to three, showing that the residual error distribution was normal with zero mean (Fig. 1). Fine tuning of the noise covariance matrix (Q) of the system and the measurement noise covariance matrix (R) is a key

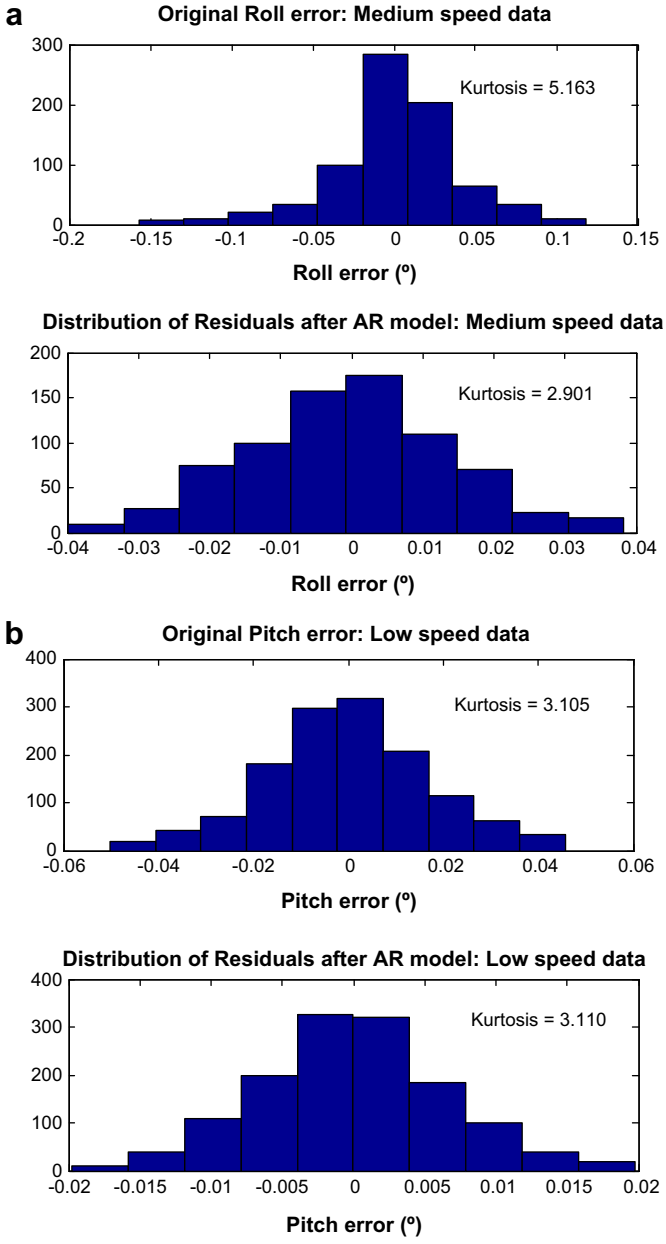

Fig. 1 – (a) Original TCM roll and (b) GPS-based pitch error distributions along with their residual error distributions after AR modelling.

process in improving the performance of an optimal, recursive DKF algorithm. In this research, fine tuning of the DKF Q matrix was straightforward since the R matrix values had already determined by the AR error modelling. The residual error, following AR modelling of the roll and pitch angle estimates, which had Gaussian error distribution, was used as a measure of noise covariance (R) in the Kalman filter implementation (Eqs. (15) and (16)). Roll and pitch angles, along with corresponding errors, were considered as the system states in the DKF implementation. Eq. (14) was the system noise covariance matrix used during DKF implementation. System noise covariance Q was calculated for different angle error values and it was observed that the performance of the DKF for both speed data was better at the angle error of 0.011°, i.e., at the error covariance value of $(\sigma_{\mathrm{DEM}})^2 = 3.68\mathrm{e}^{-8}$. The projected error covariance estimates were observed during filtering implementation to analyse the stability and convergence of the DKF. The projected error covariance estimates during DKF implementation increased initially and then converged to almost constant error covariance estimate.

The system noise covariance matrix, Q, was then defined as

$$Q = \begin{pmatrix} 3.68\times10^{-8} & 0 & 0 & 0 & 0 & 0 \\ 0 & 3.68\times10^{-8} & 0 & 0 & 0 & 0 \\ 0 & 0 & 3.68\times10^{-8} & 0 & 0 & 0 \\ 0 & 0 & 0 & 3.68\times10^{-8} & 0 & 0 \\ 0 & 0 & 0 & 0 & 3.68\times10^{-8} & 0 \\ 0 & 0 & 0 & 0 & 0 & 3.68\times10^{-8} \end{pmatrix} \quad (14)$$

The measurement noise covariance matrix was defined as the AR model covariance values as given in Table 1. At low speed, the measurement noise covariance matrix was

$$R = \begin{pmatrix} 1.12\times10^{-4} & 0 \\ 0 & 1.23\times10^{-4} \end{pmatrix} \quad (15)$$

At medium speed, the measurement noise covariance matrix was

$$R = \begin{pmatrix} 3.80\times10^{-4} & 0 \\ 0 & 3.04\times10^{-4} \end{pmatrix} \quad (16)$$

The noise covariance for the roll and pitch angle rates from DEM estimates, which was used as an input during the state estimation process, was fine tuned for various values from 0.01° s^{-1} to 3° s^{-1} to have improved DKF estimation process. Normally, the roll and pitch rate input noise covariance was taken as $(\sigma_\phi)^2 = (\sigma_\theta)^2 = (0.2^\circ\ \mathrm{s}^{-1})^2 = 1.22\mathrm{e}^{-5}$ (radian s^{-1})^2. The input noise covariance had higher influence on the DKF estimation process. An out-of-bound situation with the DEM data is the state where the DEM does not provide the attitude estimates for the vehicle. DKF state estimations need to account for the out-of-bound situation because these situations have zero values for the roll and pitch angle measurements. For the out-of-bound situation, input noise covariance was tuned to higher values so that the DKF could moderately follow the TCM-based roll and GPS-based pitch measurements instead of DKF estimates during the DKF estimation updating stage. The input noise covariance (Γ) matrix for normal situation was

$$\Gamma = \begin{pmatrix} 1.22\times10^{-5} & 0 \\ 0 & 1.22\times10^{-5} \end{pmatrix} \quad (17)$$

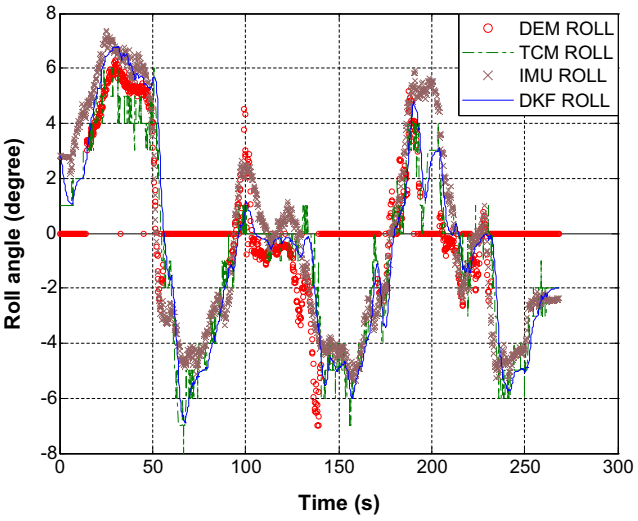

Fig. 2 – Roll angle from DEM, TCM, IMU and DKF for low speed of the sprayer vehicle. ○ DEM roll, - - - TCM roll, × IMU roll, — DKF roll.

The input noise covariance (Γ) matrix for out-of-bound situation was tuned to $(\sigma_\phi)^2 = (\sigma_\theta)^2 = (1.5^\circ\ \mathrm{s}^{-1})^2 = 6.85\mathrm{e}^{-4}$ (radian s^{-1})^2:

$$\Gamma = \begin{pmatrix} 6.85\times10^{-4} & 0 \\ 0 & 6.85\times10^{-4} \end{pmatrix} \quad (18)$$

For roll and pitch angle estimates of the sprayer from DEMs, the straight lines of zero readings on the DEM roll and pitch plots (Figs. 2 and 3) show that the sprayer was out-of-bound, i.e., no DEM data is available. Out-of-bound circumstances does not provide the roll and pitch angle estimates from the DEM, and therefore the DKF algorithm has to rely on the TCM roll measurements and single GPS-based pitch estimates to improve the attitude estimates of the

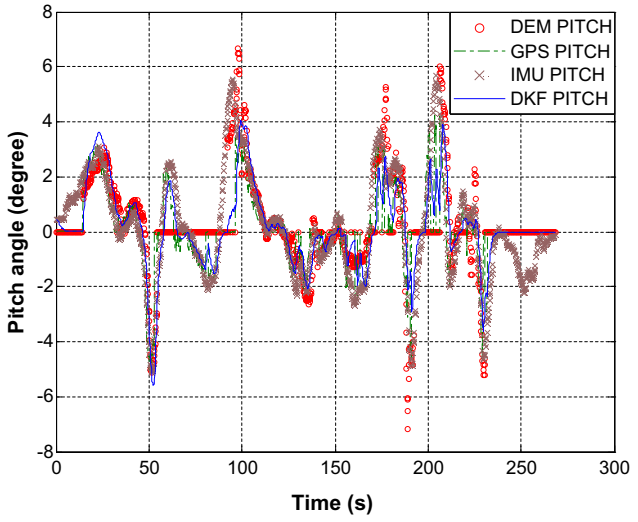

Fig. 3 – Pitch angle from DEM, GPS, IMU and DKF for low speed of the sprayer vehicle. ○ DEM pitch, - - - GPS pitch, × IMU pitch, — DKF pitch.

Table 2 – Roll and pitch error from different sources compared to DKF with IMU as a reference

Sprayer path		Roll error (°)		Pitch error (°)	
		Mean	Std. dev.	Mean	Std. dev.
Low speed	DEM	0.621	2.819	0.081	1.371
	TCM roll	−0.590	1.422		
	GPS pitch			−0.081	1.436
	DKF	−0.419	1.364	0.006	1.225
Medium speed	DEM	−0.060	2.706	−0.003	1.670
	TCM roll	−0.032	2.286		
	GPS pitch			−0.002	1.973
	DKF	0.018	2.190	0.007	1.901

sprayer during the DKF estimation process. This situation could be related to that of the GPS outage situation where an EKF uses inertial measurements to estimate the position of an autonomous vehicle (Guo *et al.*, 2003). The DKF algorithm was effective in estimating the attitude angles for the out-of-bound circumstances which can be seen in Figs. 2 and 3. Moreover, DKF estimated roll and pitch angles were close to the IMU measurements though the DEMs estimates were absent or differed from the IMU measurements. TCM roll angle measurements (Fig. 2) and single GPS-based pitch angle estimates (Fig. 3) were close to the reference IMU measurements but had high-frequency noise associated with them. The DKF algorithm was successful in removing the noise from these sources which is evident from Figs. 2 and 3, respectively.

The roll and pitch angle errors from different sensor sources were obtained, considering the IMU measurements as the standard reference (Table 2). For the low and medium speed data, the mean roll errors from the DKF estimates (−0.419° and 0.018°) were considerably lower when compared to the mean roll errors from TCM (−0.590° and −0.032°) and the mean DEM roll angle errors (0.621° and −0.060°). Additionally, for low-speed data, the DKF estimated pitch angles had a lower mean error than from the DEM- and GPS-based pitch measurements. The out-of-bound situation affected the DEM-estimated roll and pitch, providing a lower mean and higher standard deviation values of the error.

The standard deviation of the roll error was always lower for DKF estimates (1.364° and 2.190° for low and medium speeds, respectively) compared to the standard deviation of the roll error from other sensors (2.189°, 1.422° for the low speed and 2.706°, 2.286° for the medium speed with the DEM and TCM sensors, respectively). The standard deviation of the pitch error from the DKF estimates was considerably lower for low-speed data whereas for the medium-speed data, it was higher compared to the other sensor measurements. For medium-speed pitch estimates using DKF, though the standard deviation was higher, DKF considerably reduced the high frequency error associated with GPS-based pitch estimates and the estimates were smoother and continuous when compared to that of DEM-estimated pitch. For both the speeds, DKF was able to overcome the out-of-bound situation caused from DEM and also during that period DKF estimates were smoother compared to complimentary sensors used for fusion.

Thus, DKF was effective in improving the attitude estimates of the self-propelled sprayer when compared to the measurements from individual sensors, namely, DEM, TCM and RTK-GPS. Additionally, the DKF was able to overcome the out-of-bound situation (data outage) occurred in DEM while estimating the attitude of the self-propelled sprayer. Thus, the use of DEM-based attitude estimates along with other cost-effective sensors would reduce the cost of the additional sensors commonly used for accurate attitude estimation.

4. Conclusions

From this research, the following conclusions can be drawn:

(1) The developed roll–pitch DKF algorithm was effective in improving the attitude angle estimates of the self-propelled sprayer by fusing the DEM-based roll and pitch estimates with the TCM-based roll measurements and a single RTK-GPS-based pitch estimates, respectively.
(2) The DKF algorithm was effective in estimating the sprayer attitude angles even when the DEM attitude estimates were not available for certain period due to the self-propelled sprayer being out-of-bound of the DEM.

The AR modelling of the attitude angle measurement errors improved the quality of DKF implementation as it generated residual errors that were more close to true white Gaussian noise, which also led to more effective filter tuning. The DKF algorithm along with AR modelling was effective in removing the high frequency and Gaussian noise associated with the TCM and GPS sensor measurements. In conclusion, the fusion algorithm was found to be effective in improving attitude estimate of the self-propelled agricultural sprayer, which can be extended to facilitate the automatic control of the implements that interact with the soil surface on an undulated topographic surface.

REFERENCES

Babu R; Wang J (2004). Improving the quality of IMU-derived Doppler estimates for ultra-tight GPS/INS integration. In: GNSS2004, International Conference, Rotterdam, The Netherlands, 16–19 May.

Barut M; Bogosyan S; Gokasan M (2007). Speed-sensorless estimation for induction motors using extended Kalman filters. IEEE Transactions on Industrial Electronics, **54**(1), 272–280.

Bergeijk V J; Goense D; Keesman K J; Speelman L (1998). Digital filters to integrate Global Positioning System and dead reckoning. Journal of Agricultural Engineering Research, **70**(2), 135–143.

Brockwell P J; Davis R A (1996). Introduction to Time Series and Forecasting. Springer-Verlag New York Inc., New York.

Broersen P M T; De Waele S (2005). Automatic identification of time-series models from long autoregressive models. IEEE Transactions on Instrumentation and Measurement, **54**(5), 1862–1868.

Clark R L; Lee R (1998). Development of topographic maps for precision farming with kinematic GPS. Transactions of the ASAE, **41**(4), 909–916.

Colvocoresses A P (1993). GPS and the topographic map. Photogrammetric Engineering and Remote Sensing, **59**(11), 1593–1594.

Djuric P M; Kay S M (1993). Order selection of autoregressive models. IEEE Transactions on Signal Processing, **40**(11), 2829–2833.

Grewal M S; Weill L R; Andrews A P (2001). Global Positioning Systems, Inertial Navigation and Integration. John Wiley & Sons, Inc., New York.

Guo L S; Zhang Q; Feng L (2003). A Low-cost Integrated Positioning System of GPS and Inertial Sensors for Autonomous Agricultural Vehicles. ASABE Paper No.03-3112. ASABE, St. Joseph, Michigan, USA.

Hong H; Lee J G; Park C G; Han H S (1998). A leveling algorithm for an underwater vehicle using extended Kalman filter. IEEE Position Location and Navigation Symposium. Palm Springs, California, USA, 20–23 April.

Kallapur A G; Anavatti S G (2006). UAV linear and nonlinear estimation using extended Kalman filter. In International Conference on Computational Intelligence for Modelling Control and Automation, and International Conference on Intelligent Agents. Web Technologies and Internet Commerce, Sydney, Australia. 29 Nov–1 Dec.

Khot L R; Tang L; Blackmore S; Nørremark M (2006). Navigational context recognition for an autonomous robot in a simulated tree plantation. Transactions of the ASAE, **49**(5), 1579–1588.

Kiriy E; Buehler M (2002). Three-state Extended Kalman Filter for Mobile Robot Localization. CIM Technical Report, TR-CIM 05-07. Electrical and Computer Engineering, McGill University, Montréal, Canada.

Kise M; Zhang Q (2006). Sensor-in-the-loop tractor stability control: look-ahead attitude prediction and field tests. Computers and Electronics in Agriculture, **52**(1–2), 107–118.

Liew V K (2004). On autoregressive order selection criteria. Computational Economics, Paper No. 0404001, Economics Working Paper Archive, accessed on January, 2006, Available from: <http://129.3.20.41/eps/comp/papers/0404/0404001.pdf>.

Padulo P; Arbib M A (1974). System Theory: A Unified State-space Approach to Continuous and Discrete Systems. Saunders, Philadelphia.

Rehbinder H; Hu, X (2000). Nonlinear pitch and roll estimation for walking robots. In: Proceedings of the 2000 IEEE International Conference on Robotics and Automation, Vol. 3, pp 2617–2622.

Reid J F; Zhang Q; Noguchi N; Dickson M (2000). Agricultural automatic guidance research in North America. Computers and Electronics in Agriculture, **25**, 155–167.

Wang J; Gao Y (2005). Multi-sensor data fusion for land vehicle attitude estimation using a fuzzy expert system. Data Science Journal, **4**(28), 127–139.

Wang P (1998). Applying two dimensional Kalman filtering for digital terrain modelling. In: ISPRS Commission IV Symposium on GIS - Between Visions and Applications, Stuttgart, Germany, Vol. 32(4), pp 649–656.

Westphalen M L; Steward B L; Han S (2004). Topographic mapping through measurement of vehicle attitude and elevation. Transactions of the ASAE, **47**(5), 1841–1849.

Woods J W; Radewan C H (1977). Kalman filtering in two dimensions. IEEE Transactions on Information Theory, **23**(4), 473–482.

Xiang Z; Ozguner U (2005). A 3D positioning system for off-road autonomous vehicles. IEEE Proceedings on Intelligent Vehicles Symposium 130–135.

Yao H; Clark R L (2000). Development of topographic maps for precision farming with medium accuracy GPS receivers. Transactions of the ASAE, **16**(6), 629–636.